Journal of Civil Engineering and Construction 2023;12(2):86-99
https://doi.org/10.32732/jcec.2023.12.2.86

Evaluation of Performances of Calcined Laterite and Oyster Shell Powder Based Blended Geopolymer Binders

Ludovic Ivan Ntom Nkotto[1,2,*], Lionel Jacques Ntamag[1], Frances Jane Manjeh Ma-A[1], Judicaël Sandjong Kanda[3], Jordan Valdès Sontia Metekong[1,*]

1. Laboratoire d'Analyses des Matériaux, Mission de Promotion des Matériaux Locaux (MIPROMALO), BP 2393, Yaoundé, Cameroun
2. Laboratoire en Engineering Civil et Mécanique, Ecole Nationale Supérieure Polytechnique de Yaoundé, BP 8390, Yaoundé, Université de Yaoundé 1, Cameroun
3. Laboratoire de Recherche sur les Risques Naturelles, Direction de la Recherche, Institut National de la Cartographie(INC), BP 157, Yaoundé, Cameroun
E-mail: ludovicivan.li@gmail.com; jordansontia@gmail.com

Received: 24 January 2023; Accepted: 28 March 2023; Available online: 5 May 2023

Abstract: This work consisted in characterizing of calcined laterite and oyster shell powder based blended geopolymer binders. To do this, raw laterite taken from Soa in the city of Yaoundé and oyster shells extracted from Mouanko in the Sanaga-Maritime were initially air-dried, then dried at 105 °C, before being calcined at 500 °C and 200 °C respectively for 2 hours. These samples were subjected to preliminary studies, i.e. determination of their chemical and mineralogical compositions, particle size distributions, densities, as well as thermal analysis for the synthesis of geopolymer binders. X-ray diffractometry, thermal and gravimetric analysis were carried out on the oyster shell powder and laterite, in order to elucidate the time and degree of calcination of the two samples, the evolution of the linear shrinkage, the setting time as well as the compressive and flexural strengths of the geopolymer binders. The results obtained show that oyster shells are rich in $CaCO_3$ and contain crystalline phases, while laterite is rich in silica, iron ($FeCO_3$) and alumina (Al_2O_3). The geopolymer samples: Lat + 0% oyster shells have a setting time between 125 and 168 min for a compressive strength of about 47 MPa. The peak strength is observed around 15% addition of oyster shell powder, i.e. 53.5 MPa at 28 days with an increased setting time. This strength was decreased from 25 % of addition of oyster shells, despite the increase observed in the setting time. It appears from this study that the addition of 15% oyster shell increases the compressive strength of the geopolymer, but also leads to a considerable decrease in absorption rate. Above this rate, the compressive strength decreases drastically and concomitantly the setting time increases.
Keywords: Laterite; Oyster shells; Alkaline solution; Geopolymer binder; Physico-chemical properties.

1. Introduction

Hydraulic binders play an increasingly important role in human development and activities through the production of various types of concrete. Among these, Portland cement remains the most widely used despite the fact that it is energy intensive. Indeed, the manufacture of one tonne of clinker requires about 4200 kJ because of the high temperatures required (1450 to 1500 °C) and generates about one tonne of CO_2 as well as other gases such as NOx and SOx responsible for the greenhouse effect and acid rain [1]. It is estimated that more than 3.2 billion tonnes of cement are produced per year worldwide. This production could reach 5 billion tons by 2030 to 2050 [2-3]. Hence the need to develop less expensive and environmentally friendly hydraulic binders. It is in this perspective that this work will focus on the characterization of composite materials with a cementitious matrix called geopolymers (based on calcined laterite and oyster shell powder) that can be used in fields such as civil engineering. These materials are obtained as a result of geosynthesis (geopolymerisation) involving natural or synthetic aluminosilicates and in which amorphous silicon and aluminium oxides react in a strongly basic medium to form edifices that are chemically and structurally comparable to natural rock [1]. The resulting products have superior properties to those of hitherto known binders: low setting and shrinkage times, high heat and fire resistance, resistance to chemical attack and good compressive strength [1,4]. Calcined laterite powder as well as metakaolin is a pozzolanic component rich in both silica and alumina and leads to alkaline activation of materials with remarkable properties. However, its addition with oyster shell powder, rich in alumina and calcium oxide during the synthesis of geopolymer binders, can also optimize their properties [5-8].

The objective is to find the optimal formulation content of the geopolymer based on calcined laterite, oyster shell and silicate based on rice husk ash according to its physical and mechanical characteristics. This work is part of a framework for the valorization of local and available resources in the environment for the development of ecological materials respectful of the environment.

2. Materials and methods

2.1 Materials

The basic materials used in the formulation of the geopolymer were: silicate from rice husk ash + soda (an alkaline solution), calcined laterite (an aluminosilicate material), oyster shells (a source of calcium oxide).The laterite used (**Fig.1**) was extracted in the city of Yaoundé, in the Méfou-et-Afamba Division, district of Soa, more precisely in the Nkolfoulou neighborhood. The geographical coordinates of this deposit are: 3°55'0"North and 11°34'60" East longitude, in DMS (degree, minute, second) or 3.91667 and 11.5833 in DD.

Fig.1. Deposit of laterite

The oyster shells designated **OS** (**Fig.2**) were collected in Mouanko (Division of Sanaga Maritime, Littoral Region, Cameroon), a locality located about 100 km from the city of Douala and having geographical coordinates 10°E and 3°30'N. In Mouanko, oysters are fished for their flesh and the shells collected in tens of thousands of tons are dumped in the waters of the Sanaga, spread on the muddy surfaces of housing areas, tracks or simply dumped in heaps. Today, they are beginning to be used in the formulation of poultry feed, in ceramics and decoration, but also timidly as an industrial raw material for construction materials.

Fig. 2. Deposit of oyster shells

Oyster shells were collected from a landfill site **(Fig. 2)**. The shells were washed and dried at 105 °C for 24 hours before being ground and sieved to 75µm. After grinding, the powder obtained was calcined at 200 °C. This powder was gradually substituted for laterite in the formulation of the geopolymer binder (**Fig. 3a and 3b**).

The alkaline solution is a mixture of aqueous sodium hydroxide and silicate solution. The sodium hydroxide solution of molarity 6 M is obtained by dissolving in distilled water caustic soda flakes having a purity of 99 %. The sodium silicate was obtained by preparing the sodium hydroxide solution with rice husk ash.

The rice husk ash (RHA)/NaOH activator was prepared by adding a 6 M NaOH solution to the as-collected rice husk ash (RHA) at a solid/liquid ratio from equation **(1)** in accordance with the research work of Venyite et al. [9]. The mixture was then heated in a silver cookware at 100 °C for 2 h and the final product obtained was a dark grey viscous gel (**Fig. 3c**). The main reactive constituent of RHA is assumed to be silica which constitutes about 98% of RHA [10]. The equation below represents the reaction of silicate gel formation from NaOH and silica [11].

$$\underset{Soda}{2NaOH\,(aq)} + \underset{RHA}{xSiO_2} \xrightarrow{(100\,℃)} \underset{silicate\ gel}{Na_2O(SiO_3)} + \underset{Wate}{H_2O} \quad \textbf{(1)}$$

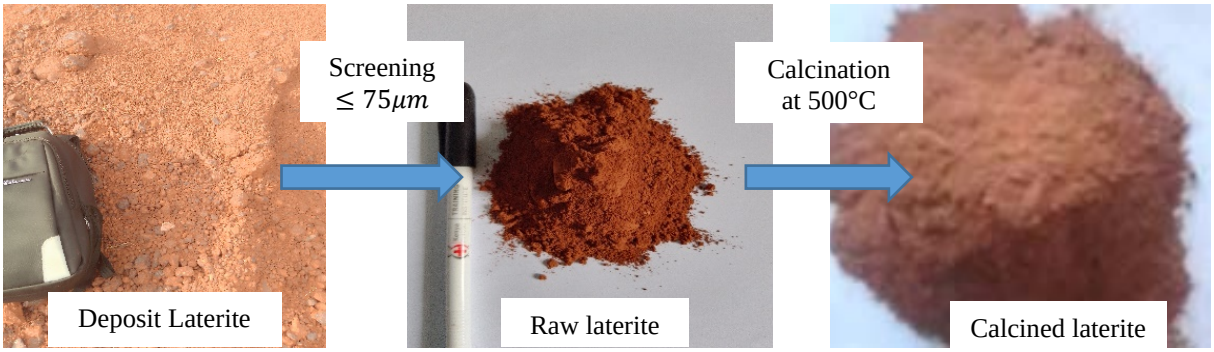

Fig. 3a. Preparation of laterite

Fig. 3b. Preparation of oyster shellS

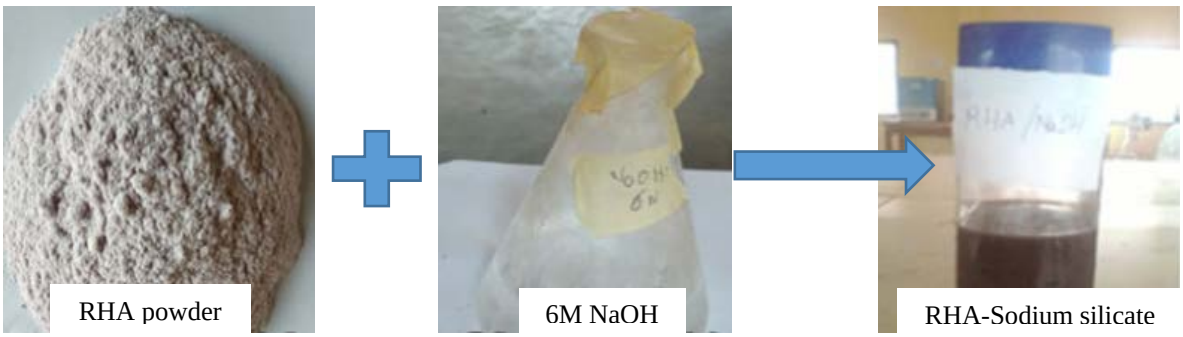

Fig. 3c. Alkaline solution preparation

Fig. 3. Sample formulation steps

The resulting silicate gel was stored in closed bottles and kept for 48h before use [12]. It was then mixed with 8 M NaOH in a volume ratio of 2:1 and used in geopolymer synthesis. The preparation of our raw material followed the following steps:

1) Extraction and pre-treatment of laterite, then grinding to 75µm and calcination at 500 °C;

2) Extraction and pre-treatment of oyster shells, followed by grinding to 75 µm and calcination at 200 °C;
3) Extraction and pre-treatment of rice husks followed by grinding and pulverising to 75 µm;
4) Preparation of the alkaline solution;
5) Formulation of the specimens at different percentages.

2.2 Geopolymer's formulation

Fig. 4 shows the process of developing geoplymer binders through to characterization. The geopolymer binder samples (calcined laterite + calcined oyster powder) were obtained by progressive substitution of laterite for calcined oyster powder at different rates for a total mass of 300g with the alkaline solution in a constant mass ratio liquid/solid (L/S) of 0.7 (**Table 1)**. The mixtures were mixed in a mixer (M & O, model N50- G) for 5min. Part of the fresh paste obtained is used for the determination of the setting time and the other part is poured into cylindrical PVC moulds for linear shrinkage and compressive strength measurements (diameter = 20 mm, height = 40 mm). The resulting specimens were manually vibrated for 2 min to remove air bubbles trapped during casting. The resulting specimens were covered with a thin polyethylene film and then left at the ambient temperature of the laboratory (24 ± 3 °C). Demoulding took place 24 hours after casting.

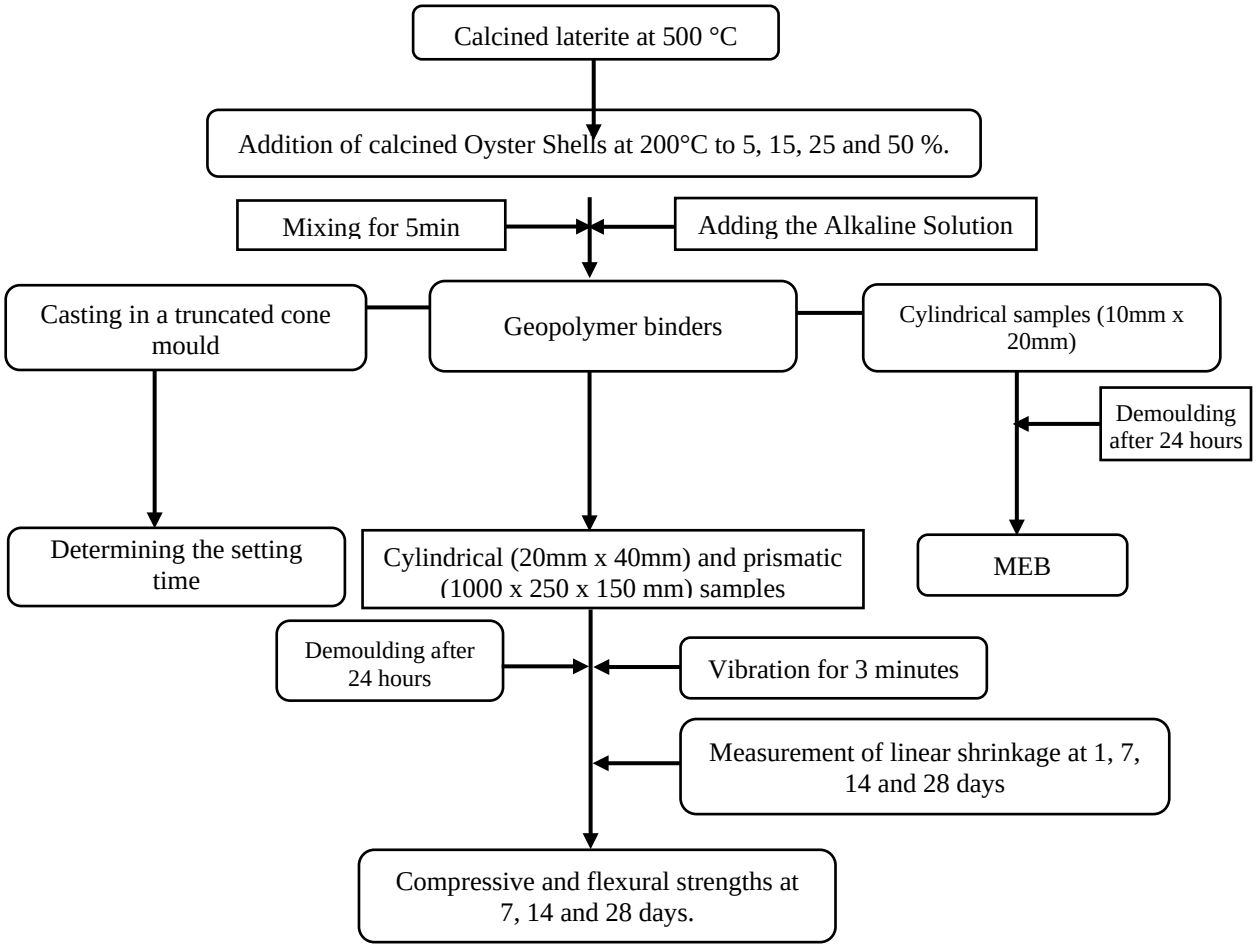

Fig. 4. Experimental protocol for the development and characterization of the materials studied

Table 1. Formulation of specimens

Formulations	Calcined laterite (g)	Calcined oyster shells (g)	Total mass (g)	Liquid/solid ratio	Number of specimens
LAT	300	0	300	0.7	4x2
LAT+5%OS	285	15	300	0.7	4x2
LAT+15%OS	255	45	300	0.7	4x2
LAT+25%OS	225	75	300	0.7	4x2
LAT+50%OS	150	150	300	0.7	4x2

2.3 Method of characterization

Several analytical methods were set up in this study. Physical, chemical and thermal analysis for the inputs and physical and mechanical analysis for the formulated geopolymer binders.

2.3.1 Particle size analysis, Atterberg limits, methylene blue, actual density, bulk density, setting test

The particle size analysis was carried out on the laterite using two standard procedures by dry sieving of the sample previously washed, steamed at 105°C and sieved through standardized sieves in accordance with the procedure of the French standard NF P 94-056 for particles greater than 80 μm. For particles smaller than 80 μm, it was done by sedimentometry following the protocol of the French standard NF P 94-057.

The Atterberg limits of laterite were evaluated. The liquidity limit ω_L, the plasticity limit ω_P and the plasticity index **IP** were deduced according to the procedure of the French standard NF P 94-051 in order to find the water content for which a groove of standardized dimensions, made in the soil placed in a Casagrande cup closes under the action of 25 shocks applied in a standardized manner and to find the water content for which a manually made soil roll of diameter 3 mm and length 10 to 15 cm cracks when lifted.

The methylene blue test was carried out on the laterite steamed at 105 ± 5 °C for 24 hrs in order to evaluate the quantity and quality of the clay fraction contained in the said laterite following the protocol of the French standard NF P94-068.

The real density and the apparent density were carried out on both the laterite and the oyster shell powder in accordance with the procedures of the ASTM C 373 standard [13].

The setting test was carried out in accordance with EN 196-3 using the Vicat instrument, which in a chamber where the temperature is maintained at 24 ± 3 ºC. The penetration of a needle with a diameter of 1.13 attached to the mobile part of the Vicat apparatus, with a total mass of 300 g, into a pure paste of cement held in a truncated cone-shaped mould 40 mm high, is measured. When the needle stops at a distance d = 4 ± 1mm from the flat base plate, the time of the start of setting is recorded. The end of setting is the time when the needle no longer penetrates the ring [14], i.e. a smooth and gradual transformation of the cement paste into a rigid block.

2.3.2 Chemical analysis

Chemical analysis uses a set of procedures and techniques to identify and quantify the elements present in a sample of material. It was carried out by alkaline fusion of the sample with lithium metaborate LiBO followed by recovery in concentrated nitric acid. Subsequently, the major elements were determined by ICP AES (Inductive Coupled Plasma- Atomic Emission Spectrometry). This technique uses a partially ionised argon source at very high temperature (4500 to 6000 kJ) as an excitation medium. The elements to be measured can be introduced from solutions or suspensions of fine particles (< 1). The loss on ignition is measured by calcination the material at 1000 °C. These chemical analyses, carried out on the lateritic fraction (**LAT**) and Oyster Shells (**OS**), carried out in the Laboratory of Materials Analysis of the Demo-Center of the University of Modena and Reggio Emilia (Italy).

2.3.3 Thermal analysis

Differential scanning calorimetry (DSC), coupled with thermogravimetric analysis (TGA), has made it possible to highlight changes in the physicochemical states of compounds subjected to temperature variations. These changes are manifested by exothermic or endothermic phenomena. Differential scanning calorimetry measures the evolution of the temperature and energy difference between the sample and an inert control body, thus indicating the various thermal phenomena. Thermogravimetric analysis measures the decrease in mass as a function of temperature and provides information on the various thermal reactions that take place in the initial material. These analyses, carried out on laterite powders (**LAT**) and oyster shells (**OS**), were carried out on a Linseis STA PT1000, whose SiC-type furnace is equipped with the ATG/DSC head, which allows a maximum temperature of 1000 °C to be reached at a heating rate of 20 °C/min. These analyses were carried out in the Laboratory of Inorganic Chemistry of the University of Yaoundé 1.

2.4 Physical properties

2.4.1 Water absorption

The aim of this test is to determine the mass percentage of water absorbed by our geopolymer samples during a 24-hour period. The amount of water absorbed was deduced from the mass difference before and after soaking of our geopolymers during these 24 hours. The procedure was carried out in accordance with ASTM C373-14 [13].

2.4.2 Compressive and flexural strengths

The mechanical bending strength was determined through samples of dimensions 40×40×160 mm by means of a material characterization apparatus equipped with a three-point bending device. The handling and handling

conditions are described according to EN 196-1 and the flexural strength σ_f (in MPa) is obtained from the equation **(2)**.

$$\sigma_f = \frac{3}{2} \times \left(\frac{F \times L}{b \times h^2}\right) \quad \textbf{(2)}$$

Where **F** load applied at the centre (N), **L** length between supports (mm), **b** the width of the specimen (mm) and **h** the height of the specimen (mm).

In order to deduce the compressive strength of our geopolymer materials, the half-prisms of the previously used 40 × 40 × 160 mm flexural specimens were reused [15] . The specimens were subjected to simple compression to crushing using a compression test press and the compressive strength σ_c is obtained according to the equation **(3)**.

$$\sigma_C = \frac{F}{S} \quad \textbf{(3)}$$

Where **F** compressive force at break in N and **S** area of application of the force in mm^2.

3. Results and discussion

3.1 Chemical characteristics of the inputs

The chemical composition of oyster shells (**OS**) is presented in **Table 2**.

Table 2. Chemical composition of oyster shells

Sample	SiO_2	Al_2O_3	Fe_2O_3	CaO	MgO	SO_3	K_2O	Na_2O	P_2O_5	PaF	Total
OS	0.39	0.21	0.1	55.23	0.21	0.06	0.05	0.48	0.19	43.08	100

The X-ray diffractogram of oyster shells (**OS)** (**Fig. 5**) shows that it consists only of Calcite ($CaCO_3$), lines at (in): 3.89; 3.03; 2.84; 2.50; 2.28; 2.10; 1.92; 1.87; 1.58; 1.52 (PDF File 5-586) This suggests that the product obtained after heat treatment of the oyster shell is a calcite.

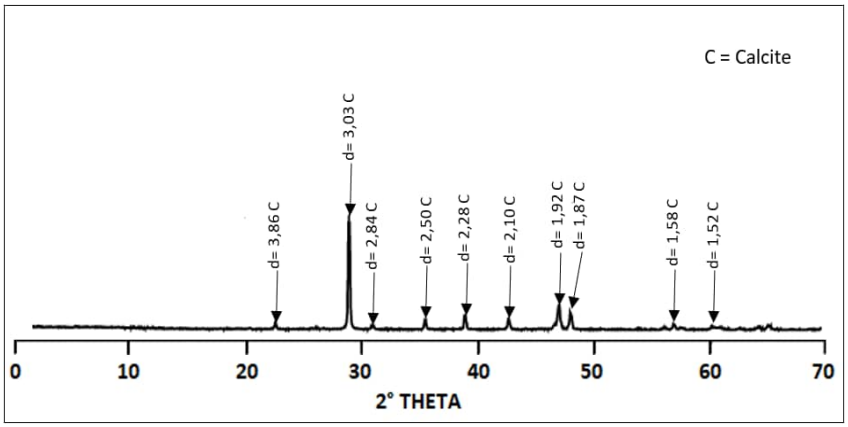

Fig. 5. X-ray diffractogram of oyster shells (**OS**)

The chemical composition of laterite (**LAT**) is presented in **Table 3**.

Table 3. Chemical composition of laterite

Sample	SiO_2	Al_2O_3	Fe_2O_3	CaO	MgO	SO_3	K_2O	Na_2O	P_2O_5	PaF	Total
LAT	20.75	19.46	45.81	0.69	0.02	0.04	0.03	0.09	0.39	12.61	99.89

The X-ray diffractogram of laterite **(Fig. 6)** shows that it consists of the following chemical compounds with their base spacing:

1) Quartz **SiO_2 =** 4.25; 3.34; 2.28; 2.24; 2.20; 2.12; 1.99; 1.81; 1.67; 1.65; 1.56; 1.45 and 1.39
2) Illite = $(K, H_3O)(Al,Mg, Fe)_2(Si, Al)_4O_{10}[(OH)_2, (OH)_2]$ **:** 4.97; 4.40; 2.68; 2.57; 2.38; 2.24 and 1.99
3) Muscovite = $KAl_2(AlSi_3O_{10})(OH,F)_2$ **:** 9.90 ; 4.97 ; 4.47 ; 2.68 ; 2.57 and 2.38
4) Hématite = Fe_2O_3 : 2.20 ; 1.84 and 1.70
5) Gibbiste = Al(OH) : 2.38 ; 1.99 and 1.78

6) Kaolinite = $2SiO_2$, Al_2O_3, $2H_2O$ **:** 7.16 ; 4.47 ; 4.13 ; 3.57 ; 2.57 ; 2.49 ; 2.34 ; 2.28 ; 1.56 ; 1.49 ; 1.39 ; 1.39
7) Montmorillonite = $(Na, Ca)_{0,3}(Al,Mg)_2Si_4O_{10}(OH)_2$. nH_2O **:** 4.47 ; 1.89 ; 1.70
8) Pyroxène = $[Si_2O_6]^{4-}$ **:** 3.12 ; 2.42
9) Goethite = Fe_2O_3+H_2O **:** 4.97 ; 2.49 ; 2.47 ;
10) Boehmite = Al_2O_3, H_2O **:** 2.34 ; 1.65

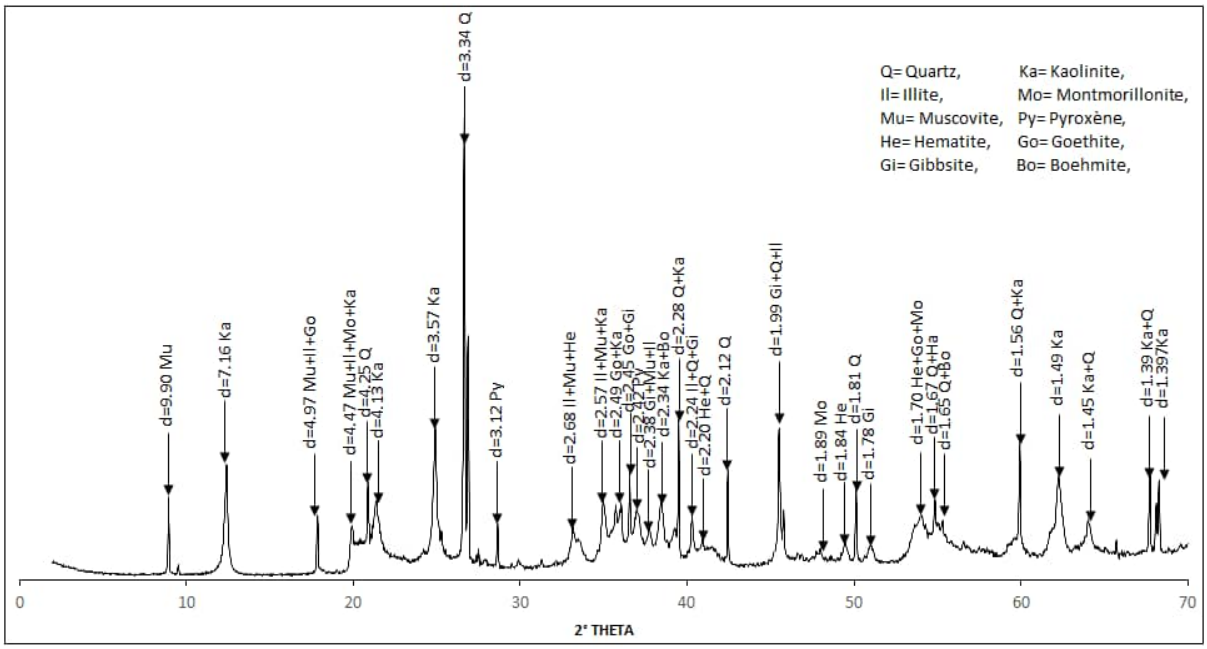

Fig. 6. X-ray diffractogram of laterite (**LAT**)

This analysis allowed us to better understand the chemical composition of our different materials, and therefore to have an idea of the different chemical reactions that will occur in the geopolymer matrix.

3.2 Thermal analysis of raw materials

3.2.1 Thermal analysis of oyster shells

This analysis was carried out at the laboratory of inorganic chemistry of the University of Yaoundé I. It allowed us to observe at least two changes in the mass variation of oyster shells (**Fig.7**):

1) The endothermic peak whose maximum is at 156 °C corresponds to the loss of free water this is justified by the loss of water and organic matter and the transformation of aroganite into calcite [16] until 650 °C;

2) The second change takes place at 749 °C this is due to the fact that calcite transforms into quick lime following the equation **(4)**:

$$CaCO_3 \rightarrow CaO + CO_2 \quad \textbf{(4)}$$

This analysis allowed us to have an exact calcination temperature for our oyster shells without changing the structure of our material. The calcination temperature used was 200 °C.

3.2.2 Thermal analysis of laterite

The TGA/DSC curves of as-received laterite (**LAT**) are shown in **Fig.8**. The DSC curve indicates four (04) thermal phenomena: the first endothermic peak at about 56 to 100 °C corresponds to the loss of physically absorbed or free water molecules. The second appearing at 283 °C is attributed to the dehydroxylation of hydroxylated compounds (such as gibbsite to boehmite) [17]. The third endothermic peak between 483 and 600 °C is related to the dehydroxylation of kaolinite to metakaolinite and the transformation of boehmite to alpha-alumina [18] and the last exothermic peak between 900 and 1000 °C corresponds to the reorganisation of the clay minerals reflecting the transformation of metakaolinite into spinel and amorphous silica. This indicates that in order to have an optimal proportion of amorphous phase from this laterite geopolymerisation reaction, the recommended calcination temperature is 501.74 °C. This laterite calcination temperature for the geopolymer is closer to the 500 °C reported by Kaze et al. [19] who worked with more iron-rich and aluminium-poor laterite, compared to the present case, with a lower aluminium and silica content.

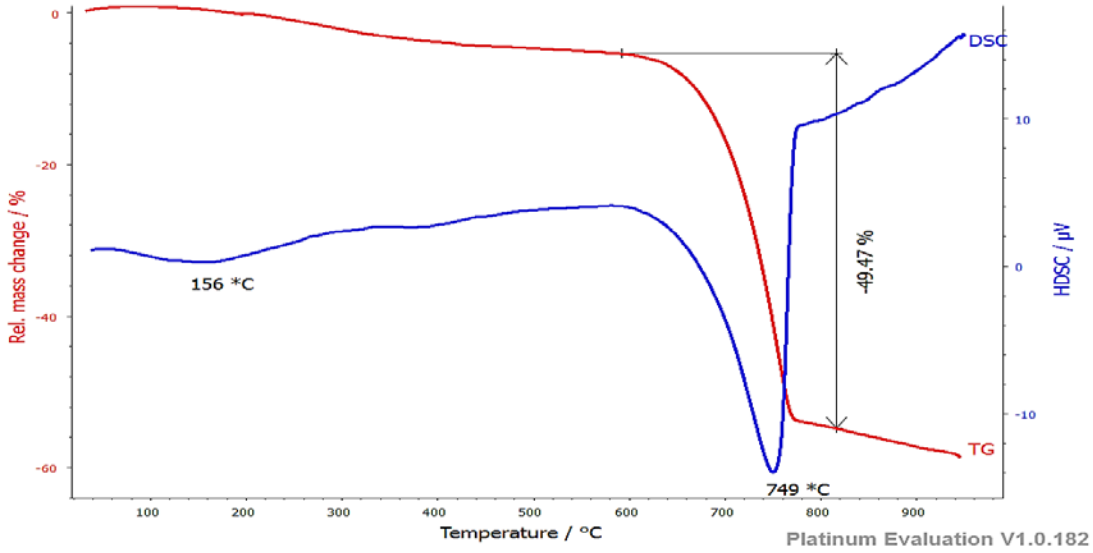

Fig. 7. DSC and TGA thermograms of oyster shells (**OS**)

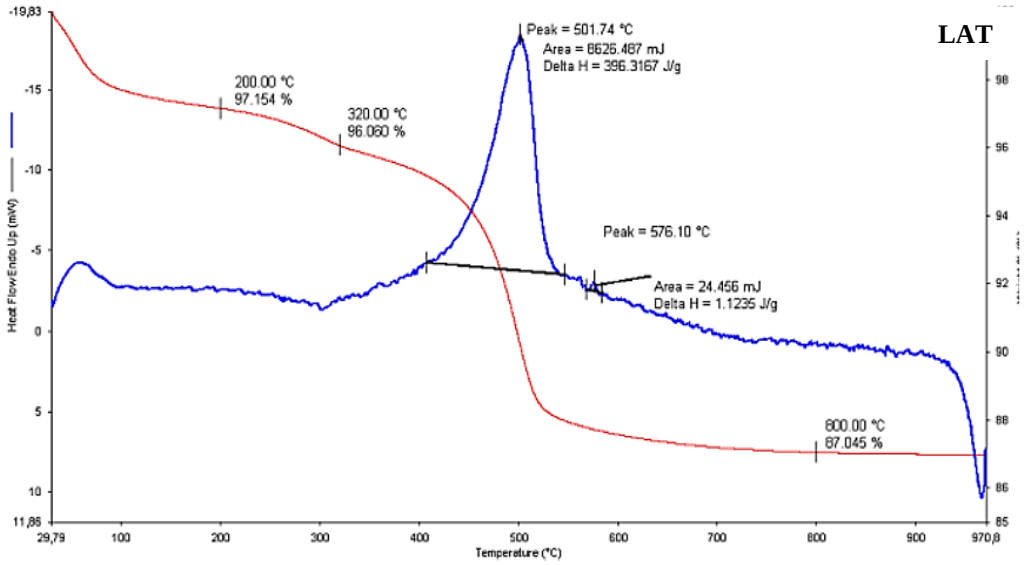

Fig. 8. DSC and TGA thermograms of laterite (**LAT**)

3.3 Physical properties

3.3.1 Particle size analysis

Computer processing of the results using Excel software gives us the particles distribution according to their size and volume occupied. The software assimilates the grains to spheres whose diameter values are given on the abscissa and refusals on the ordinate. **Fig. 9** shows the volumes occupied by the lateritic particles. Using this particle size curve, we observe that our laterite sample contains all grain classes. Hence, its decreasing shape illustrates the presence of indurate laterite and sandy particles or saprolite.

3.3.2 Atterberg limits

The Atterberg limits allowed us to determine the plasticity index, which is 28.42 %. According to the soil classification table, we can conclude that our soil is highly plastic (15 < **Ip** < 40%). This high plasticity is related to the high content of clay and quartz **(Table 4).** This is confirmed by the Methylene blue value of 0.1, corresponding to a water-insensitive soil. This suggests the presence of swelling clays in the sample.

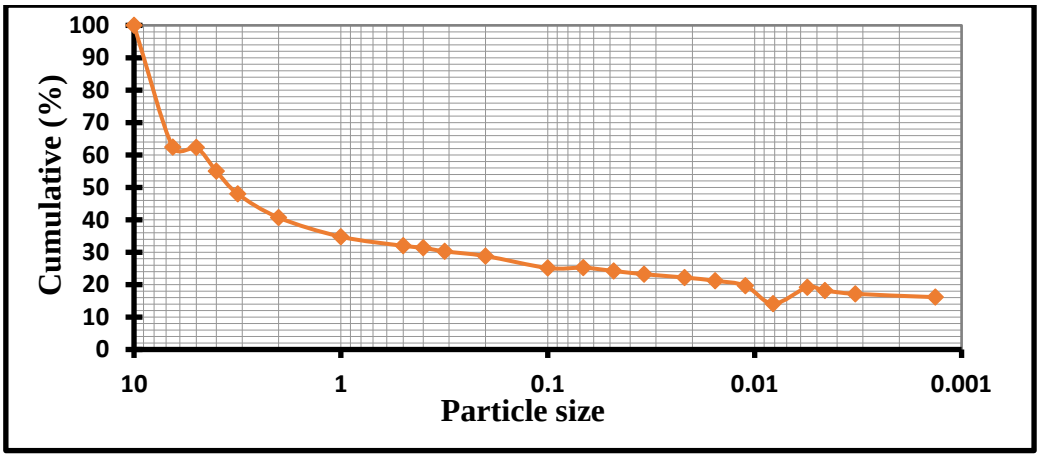

Fig. 9. Size distribution of laterite (LAT)

Table 4. Summary of the plasticity index

Sample	Liquidity limit (%)	Plasticity limit (%)	Plasticity index (%)
E1d	70.69	42.27	28.42

The consistency index is the difference between the liquid limit and the plasticity index. **Ic** is given by the equation **(5)**:

$$I_c = \frac{W_L - W}{I_P} \quad \textbf{(5)}$$

where $\mathbf{I_C}$ consistency index, $\mathbf{W_L}$ liquidity limit, $\mathbf{I_P}$ plasticity index and **W** natural water content.

For our sample, the natural water content is 5.35% per kilogram of mass, $I_c = \frac{70.69-5.35}{28.42} = 2.29$, the consistency index is 2.29 %

3.3.3 Actual and bulk density of raw materials

The apparent and real densities allow us to determine the proportion of voids in our material or its porosity. **Table 5** shows the results obtained for the determination of actual density of oyster shells. The average density of oyster shells is 0.45 g/cm^3. This shows that the volume of the material does not vary too much even after immersion in water.

Table 6 shows the results obtained for the determination of bulk density of oyster shells. The average bulk density is 2.63 g/cm^3. It is a hard, non-porous material, and occupies a very small volume, due to its irregular shape.

Table 5. Actual density of oyster shells

M1 (g)	M2 (g)	M3 (g)	M4 (g)	Dr (g/cm^3)	Average (g/cm^3)
age	165.81	641.01	665.55	0.449035	0.450796
145.81	165.81	641.01	665.13	0.453309	
145.81	165.81	641.01	665.45	0.450045	

* **M1** = mass of empty vial (g), **M2** = mass of vial with dry sample (g), **M3** = mass of flask with dry sample plus water (g), **M4** = mass of flask with distilled water filled to the mark (g), And **Dr** = actual density (g/cm^3).

Table 6. Bulk density of oysters (g/m^3)

M1 (g)	M2 (g)	V1 (cm^3)	V2 (cm^3)	mp (g)	mvp (g)	MVA (g/cm^3)	Average (g/cm^3)
9.69	9.83	300	305	0.14	0.9	2.09	2.63
18.21	18.41	300	305	0.2	0.9	3.85	
11.83	11.93	300	305	0.1	0.9	2.43	
10.6	10.78	300	305	0.18	0.9	2.23	

* **M1**= mass without paraffin (g), **M2** = mass with paraffin (g), **V1** = volume of water (cm^3), **V2** = volume after immersion (cm^3), **mp** = mass of paraffin (g), And **mvp** = density of paraffin (g/cm^3)

Table 7 shows the results obtained for the determination of actual density of laterite. The average density of laterite is 0.58 g/cm^3. This shows that the volume of the material does not vary too much even after immersion in water.

Table 7. Actual density of laterite (g/cm^3)

M1 (g)	M2 (g)	M3 (g)	M4 (g)	Dr (g/cm^3)	Average (g/cm^3)
98.49	118.02	355.62	369.84	0.58	0.58
98.49	118.02	355.62	369.77	0.58	
98.49	118.02	355.62	370.05	0.58	

* **M1** = mass of empty vial (g), **M2** = mass of vial with dry sample, **M3** = mass of flask with dry sample plus water, **M4** = mass of flask with distilled water filled to the mark , And **Dr** = actual density.

Table 8 shows the results obtained for the determination of bulk density of laterite. The average bulk density is 2.63 g/cm^3. It is a less porous material, and occupies a very small volume, due to the viscosity of the aggregates and particles.

Table 8. Bulk density of laterite in (g/cm^3)

M1 (g)	M2 (g)	V1 (cm^3)	V2 (cm^3)	mp (g)	mvp (g/cm^3)	MVA (g/cm^3)	Average (g/cm^3)
9.69	9.83	300	305	0.14	0.9	2.09	2.63
18.21	18.41	300	305	0.2	0.9	3.85	
11.83	11.93	300	305	0.1	0.9	2.43	
10.6	10.78	300	305	0.18	0.9	2.23	

* **M1** = mass without paraffin (g), **M2** = mass with paraffin (g), **V1** = volume of water (cm^3), **V2** = volume after immersion (cm^3), **mp** = mass of paraffin (g), And **mvp** = density of paraffin (g/cm^3)

3.4 Physical properties of geopolymer binders

3.4.1 Consistency

Consistency is the material's property to set. The consistency diagram **(Fig.10)** of our mix shows that it increases with the percentage of oyster shells added, which lengthens the setting time.

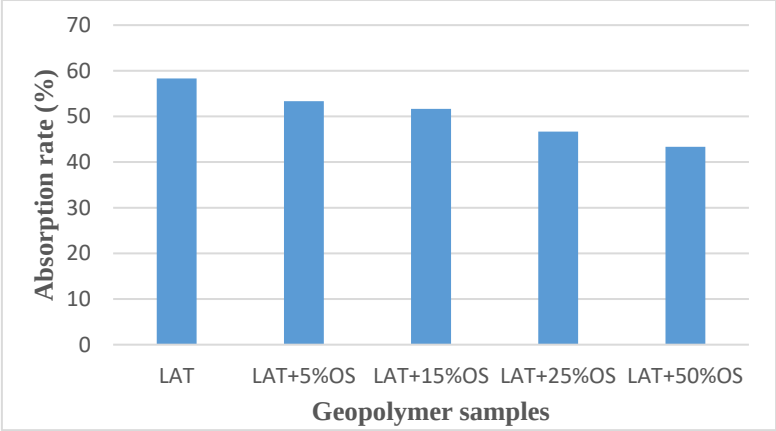

Fig. 10. Binder consistency

3.4.2 Setting time

The setting time is the time between the moment when the binder-solid mixture has been made and the moment when an increase in viscosity or stiffening of the paste, occurs (start of hardening).

The determination of the setting time according to EN 196-3 is carried out on fresh pastes of geopolymers maintained at the ambient temperature of the laboratory (24 ± 3°C). The results obtained are shown in **Fig. 11**. It appears that the setting time (initial-final) values of LAT, LAT+5%OS, LAT+15%OS, LAT+25%OS and LAT+50%OS samples were 125-168 min, 160-218 min, 220-294 min, 233-322 min and 295-418 min, respectively. For each of the formulations, the setting time increases with the percentage of admixture incorporated. These

results are similar of research work of Sontia et al.[20] who are formulated calcined laterite at 750 °C based geopolymer binders. The initial and final setting times were 120 and 150 min, respectively.

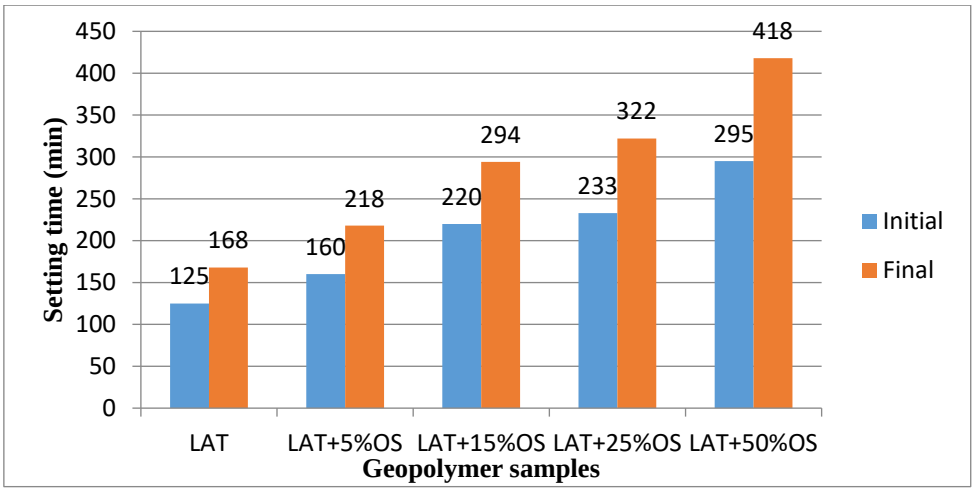

Fig. 11. Setting time

Setting time is an important phenomenon for hydraulic binders and generally depends on several parameters: the type of aluminosilicate material, its chemical composition, the fineness of its particles; the concentration of the alkaline solution, the mixing time, the dissolution rate of Si and Al, the treatment temperature [21-23]. According to the work of De Silva et al. [24] and Provis et al. [25], the setting time increases with the SiO_2 /Al_2O_3 ratio in the starting aluminosilicate material and decreases when this ratio decreases (high Al_2O_3). According to the work of Diaz et al. [26], aluminosilicate compounds with an amorphous phase, dissolve more easily than those with predominantly crystallised phases during the first stage of geopolymerisation. For laterite and oyster shells based geopolymer samples (**Fig. 11**), the time to set increases with the amount of oyster shell added. The low solubility of calcite ($CaCO_3$) contained in oyster shells does not make it easy to dissolve in alkaline solution showed that the effect of adding a calcium source during geopolymerisation depends on its crystallinity and the concentration of the alkaline solution. When calcite is used as a calcium source in the presence of a strongly basic solution, it will rather precipitate as Ca(OH) instead of dissolving. Indeed, the presence of calcium affects the geopolymerisation process by the formation of additional nucleation sites for the aluminosilicate: part of the [Al(OH)] and [SiO(OH)] complexes formed precipitate with the calcium instead of forming only the geopolymer gel, which lengthens the setting time.

3.4.3 Water absortpion

Fig. 12 shows the results obtained for the determination of water absorption of geopolymer binders. It observes that the water absorption decreases with the addition of oyster shells until the 15% turn which seems to be the peak of the mechanical strength. It starts to rise again at the 25% turn of the oyster shells. This leads to the conclusion that the optimum strength is at the 15% turn.

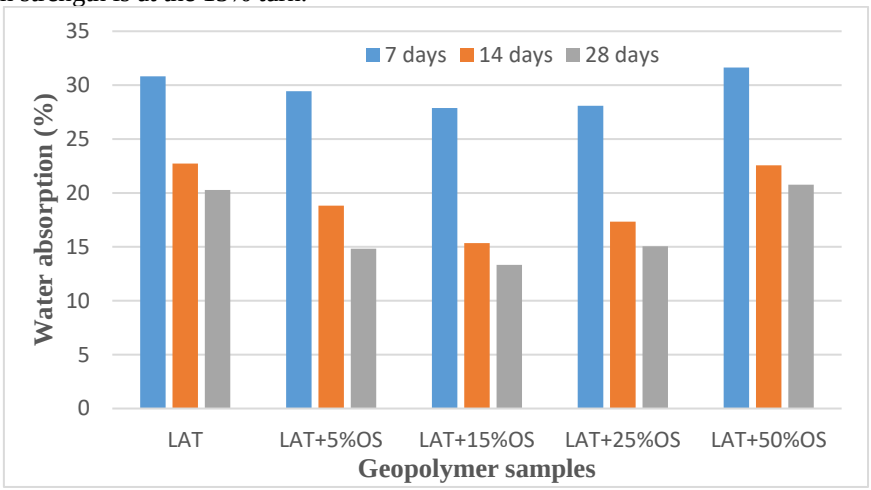

Fig. 12. Water absorption of geopolymer samples

3.5 Mechanical strengths of geopolymer samples

3.5.1 Compressive strength

Fig. 13 shows the results obtained for the determination of compressive strength of geopolymer binders. It was found that the 28-day compressive strength is highest at 15 % of the oyster shells. It was around 53.5 MPa which is higher than the strength of Ordinary Portland Cement.

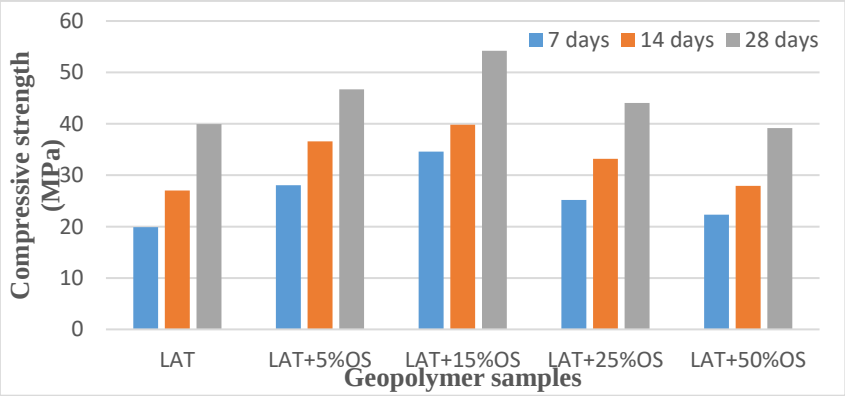

Fig. 13. Compressive strength of geopolymer samples

The compressive strength results are shown in **Fig. 13**, which presents the variations in compressive strength of geopolymer binders as a function of the percentage of admixture incorporated. The compressive strengths ranged between 39 and 54 MPa at 28 days. It was observed that the compressive strength increases considerably after incorporation of 15% oyster shell (54 MPa); beyond 15%, a decrease begins to be observed. This decrease would be due to the regression of the amorphous phase following the increase of the crystalline phase from the oyster shell. The above are shown that the incorporation of percentage of oyster shell in the calcined laterite contributes significantly to the increase in compressive strength of the geopolymer binders produced. The activation of aluminosilicates in the presence of a calcium source with a highly concentrated alkaline solution (pH>14), increases the compressive strength of the obtained geopolymers, and beyond 15 %, this addition becomes disadvantageous [5,27,28] . The minerals from the additives are crystallised and thus weakly dissolved during geopolymerisation. They have behaved as micro-aggregates and contributed to make the geopolymer matrix compact, hence the increase in mechanical characteristics. Beyond a certain percentage of additives, the quantity of crystalline phase decreases the predominance of the geopolymer gel, hence a decrease in compressive strength.

3.5.2 Flexural strength

Fig. 14 shows the results obtained for the determination of flexural strength of geopolymer binders. The maximum flexural strength was 4.3 MPa, which is obtained at 15% of the oyster shell powder. It was observed that, as in the case of compressive strength, the addition of oyster shells was increased the flexural strength up to 15%. This value was started to decrease again due to the decrease in the predominance of the geopolymer gel.

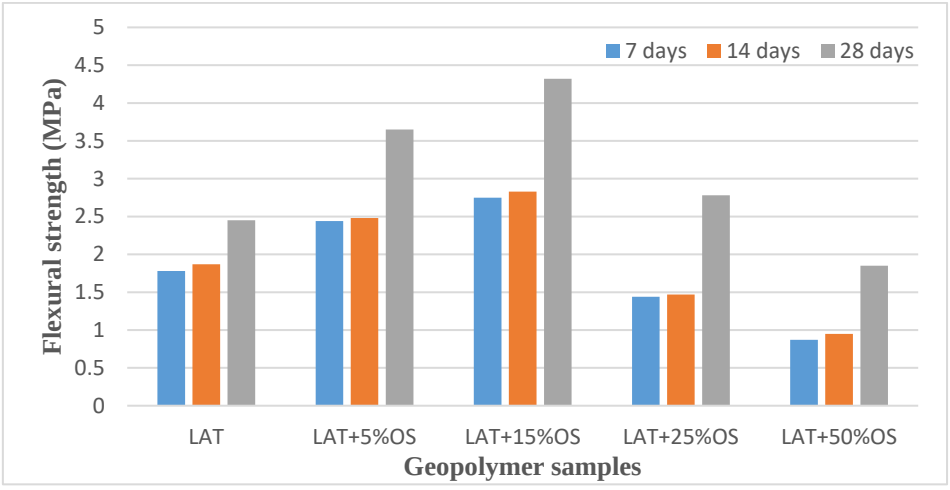

Fig. 14. Flexural strength of geopolymer samples

4. Conclusion

This study focused on the characterization of a geopolymer samples obtained from calcined laterite and oyster shell powder. It was found that the major mineral in oyster shells is calcite, and that silicon, alumina and iron are found in laterite. This study reveals the following results:

1) The addition of oyster shells compensates for the $CaCO_3$ deficit in calcined laterite, and contributes to the extension of the setting time, to allow a better geopolymerisation reaction. Thus, the presence of oyster shells in a calcined laterite-based geopolymer acts as a setting retarder;

2) Flexural and compressive strengths of laterite and oyster shells based geopolymer binders cured at 7, 14 and 28 days improve with increasing oyster shell content up to 15% but above 15% the mechanical properties deteriorate.

Based on the conclusions drawn from the results, the oyster shells are good additives as recyclable materials for the development of ecological binders for engineering applications.

Acknowledgments

The authors would like to thank the authorities of MIPROMALO for their supervision during this work.

5. References

[1] Davidovits J. Geopolymers inorganic polymeric new materials. J Therm Anal. 1991;37(8):1633–1656.
[2] Too E, Betts M, Kumar A. Sustainable Infrastructure Assets. Green Technol Concepts, Methodol Tools Appl. 2011;1034–1043.
[3] Li N, Ma D, Chen W. Projection of cement demand and analysis of the impacts of carbon tax on cement industry in China. Energy Procedia. 2015;75:1766–1771.
[4] Davidovits PJ. 30 Years of Successes and Failures in Geopolymer Applications. Market Trends and Potential Breakthroughs. 2002;1–16.
[5] Yip CK, Provis JL, Lukey GC, Deventer JSJ Van. Cement & Concrete Composites Carbonate mineral addition to metakaolin-based geopolymers. Cem Concr Compos. 2008;30(10):979–985. Available from: http://dx.doi.org/10.1016/j.cemconcomp.2008.07.004
[6] Bondar D, Lynsdale CJ, Milestone NB, Hassani N, Ramezanianpour AA. Effect of adding mineral additives to alkali-activated natural pozzolan paste. Constr Build Mater. 2011; Available from: http://dx.doi.org/10.1016/j.conbuildmat.2010.12.031
[7] Huang Y, Han M. The influence of Al2O3 addition on microstructure, mechanical and formaldehyde adsorption properties of fly ash-based geopolymer products. J Hazard Mater. 2011;193:90–94. Available from: http://dx.doi.org/10.1016/j.jhazmat.2011.07.029
[8] Tchakoute HK, Elimbi A, Mbey JA, Sabouang CJN, Njopwouo D. The effect of adding alumina-oxide to metakaolin and volcanic ash on geopolymer products: A comparative study. Constr Build Mater. 2012;35:960–969. Available from: http://dx.doi.org/10.1016/j.conbuildmat.2012.04.023
[9] Venyite P, Makone EC, Kaze RC, Nana A, Nemaleu JGD, Kamseu E, et al. Effect of Combined Metakaolin and Basalt Powder Additions to Laterite-Based Geopolymers Activated by Rice Husk Ash (RHA)/NaOH Solution. Silicon. 2021
[10] Kamseu E, Moungam L, Cannio M, Billong N, Chaysuwan D, Melo U, et al. Substitution of sodium silicate with rice husk ash-NaOH solution in metakaolin based geopolymer cement concerning reduction in global warming. J Clean Prod. 2017.
[11] Myllyam L, Mohamed H, Kamseu E, Billong N. Properties of Geopolymers Made from Fired Clay Bricks Wastes and Rice Husk Ash (RHA) -Sodium Hydroxide (NaOH) Activator. 2017;537–552.
[12] Tong KT, Vinai R, Soutsos MN. Use of Vietnamese rice husk ash for the production of sodium silicate as the activator for alkali-activated binders. J Clean Prod. 2018.
[13] ASTM C373. ASTM C373-14 Standard Test Method for Water Absorption, Bulk Density, Apparent Porosity, and Apparent Specific Gravity of Fired Whiteware Products. ASTM C373-88. 1999.
[14] Cheng TW, Chiu JP. Fire-resistant geopolymer produced by granulated blast furnace slag. 2003;16:205–210.
[15] Kubba Z, Fahim G, Rahman A, Sam M. Case Studies in Construction Materials Impact of curing temperatures and alkaline activators on compressive strength and porosity of ternary blended geopolymer mortars. Case Stud Constr Mater. 2018;9:e00205.
[16] Chan VBS, Li C, Lane AC, Wang Y, Lu X, Shih K, et al. CO2-driven ocean acidification alters and weakens integrity of the calcareous tubes produced by the serpulid Tubeworm, Hydroides elegans. PLoS One. 2012;7(8).

[17] Tchakoute HK, Rüscher CH, Djobo JNY, Kenne BBD, Njopwouo D. Applied Clay Science In fluence of gibbsite and quartz in kaolin on the properties of metakaolin-based geopolymer cements. Appl Clay Sci. 2015;107:188–194. Available from: http://dx.doi.org/10.1016/j.clay.2015.01.023
[18] Deutou N, Beda T, Biesuz M, Boubakar L, Melo U, Kamseu E, et al. Design and characterization of porous mullite based semi-vitrified ceramics. Ceram Int. 2018;44:7939–7948.
[19] Kaze RC, Beleuk MLM, Cannio M, Rosa R, Kamseu E, Chinje MU, et al. Microstructure and engineering properties of Fe2O3(FeO)-Al2O3-SiO2 based geopolymer composites. J Clean Prod. 2018;3.
[20] Sontia MJ V., Kaze CR, Adesina A, Deutou NGJ, Djobo YNJ, Lemougna NP, et al. Influence of Thermal Activation and Silica Modulus on the Properties of Clayey-Lateritic Based Geopolymer Binders Cured at Room Temperature. Silicon. 2022;18p. Available from: https://doi.org/10.1007/s12633-021-01566-7
[21] Hardjito D, Wallah SE, Sumajouw DMJ, Rangan B. Factors Influencing the Compressive Strength of Fly Ash-Based Geopolymer Concrete. Civ Eng Dimens. 2004;6(2):88–93.
[22] Rattanasak U, Chindaprasirt P. Influence of NaOH solution on the synthesis of fly ash geopolymer. Miner Eng. 2009;22(12):1073–1078. Available from: http://dx.doi.org/10.1016/j.mineng.2009.03.022
[23] Hanjitsuwan S, Silva P De, Chindaprasirt P. Effect of Speed and Time of Mixing on Setting Time and Strength of High Calcium Fly Ash Geopolymer. 2012;2012:18–21.
[24] De Silva P, Crenstel KS, Sirvisatnanon V. Kinetics of geopolymerisation: Role of Al2O3 and SiO2. Cem Concr Res. 2007;37:512–518.
[25] Provis JL, van Deventer JSJ. Geopolymerisation kinetics. 1. In situ energy-dispersive X-ray diffractometry. Chem Eng Sci. 2007;62(9):2309–2317.
[26] Diaz EI, Allouche EN, Eklund S. Factors affecting the suitability of fly ash as source material for geopolymers. Fuel. 2010;89(5):992–996. Available from: http://dx.doi.org/10.1016/j.fuel.2009.09.012
[27] Alonso S, Palomo A. Alkaline activation of metakaolin and calcium hydroxide mixtures: influence of temperature, activator concentration and solids ratio. 2001;(January).
[28] Yip CK, Lukey GC, Deventer JSJ Van. The coexistence of geopolymeric gel and calcium silicate hydrate at the early stage of alkaline activation. 2005;35:1688–1697.